ORIGINAL ARTICLE

eurosteel AMSTERDAM 2023

Ernst & Sohn A Wiley Brand

I-beam-to-SHS-column moment resisting joints using passing-through plates under equal bendings

Mouad MADHOUNI[1] | Maël COUCHAUX[1] | Mohammed HJIAJ[1] | Alper KANYILMAZ[2]

Correspondence

M.Sc., Mouad Madhouni

Institut National des Sciences Appliquées de Rennes
20 Avenue des Buttes des coesmes
35700 Rennes

Email: mouad.madhouni@insa-rennes.fr

[1] Institut National des Sciences Appliquées, Rennes, France
[2] Politecnico di Milano, Italy

Abstract

Conventional I-beam-to-SHS-column moment resisting connections are generally stiffened with external diaphragms in order to limit excessive deformation of the tube-wall. Passing through plates welded to the tube is an alternative solution that can develop significant strength and stiffness. This solution has been applied to CHS column and initial findings from RFCS project LASTEICON were encouraging. RHS columns are also widely used in practice due to simplicity of connections manufacturing. The new RFCS project LASTTS aims to investigate the application of this technique of passing through plates to SHS columns using laser cutting technology.

The objective of this paper is to present the behaviour of I-beam-to-SHS column moment resisting joints using passing-through plates under equal hogging bending moments. A finite element model using brick elements is firstly presented. This model is used to perform a sensitivity analysis varying passing through plates thicknesses as well as SHS column dimensions. The failure mode is caused by the flange plate buckling inside the tube. Analytical models are developed to determine the bending resistance and initial rotational stiffness of these connections.

Keywords

Passing-though plates, Moment resisting joints, Laser cutting technology, Tubular structures, Buckling, Finite-element modeling.

1 Introduction

In high-rise buildings, close-section members are often preferred to open-section ones in civil construction due to efficient structural behaviour and aesthetic appeal [1]. However, because of lack of accessibility, bolted beam-to-hollow section column joints are tricky to erect. I-beam-to-SHS-column moment resisting connections are generally stiffened with external diaphragms in order to limit excessive deformation of the tube-walls. Nevertheless, this solution is quite expensive and time-consuming. The solution of passing-through plates, studied within the framework of RFCS project LASTEICON [2] for CHS column, can constitute a good solution ([3], [4]) particularly in presence of gravitational loadings. The RFCS project LASTTS [5] will enlarge the scope of this research studying SHS columns. These Hollow Sections are very popular for trusses and columns, since they allow for easy connections due to their flat faces.

Under equal hogging bending moments, the potential failure can occur due to buckling of horizontal plates in compression and vertical one's in bending. Hence, the connection exhibits a clear peak load capacity. This failure has been observed experimentally [6], and numerically [7] for CHS columns.

The objective of the present paper is to characterize numerically and analytically the behaviour of I-beam-to-SHS-column joints made with passing-through plates under equal hogging bending moment. Finite element analyses are presented in section 2. The non-linear finite element model that uses brick elements is described in detail. The behaviour of joints using SHS and CHS columns are compared. In addition, a sensitivity analysis is performed to assess the effect of passing plates and columns geometry on the behaviour of the joint. An analytical model is proposed in section 3 to determine the initial rotational stiffness and bending resistance based on the model proposed for I-beam-to-CHS-column joints using passing though plates [6].

2 Finite-element model

2.1 Material properties

The mechanical properties of steel have been defined according to an elastic-plastic behaviour with kinematic hardening, adopting a Young's modulus of 210 GPa and a Poisson's ratio of 0.3. The stress-strain curve is multi-linear, based on the *true stress - true strain* curve obtained from coupon tests during LASTEICON project (see **Figure 1**). The yield stress and ultimate tensile stress are equal to 346.45 MPa and 510 MPa, respectively. The same mechanical properties have been associated to all model parts.

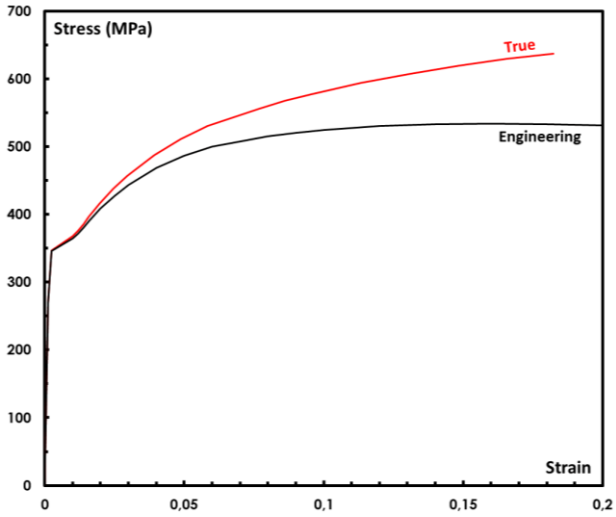

Figure 1 Steel Stress – strain curve

2.2 Joint modelling

Joints have been modelled with ANSYS 2021 R2 and analysed with non-linear static analysis. Sparse direct equation solver is used with automatic Newton-Raphson option. Furthermore, geometrical non-linearities are taken into account. 20-node solid hexahedral brick elements (SOLID186) are used. Each having three degrees of freedom per node: translations in the nodal x, y, and z directions. The general mesh layout adopts a fine mesh around the joint panel to better capture surface undulations, as well as stress and strain distributions. Moving away from the joint region, a gradual increase of element size is applied, resulting in a coarser mesh. Numerical modelling requires that at least three through-thickness elements to be used for the plates and two for the chord, otherwise results may prove excessive flaw.

To establish a connection between the SHS column and the passing elements, the two parts share the same nodes and elements at junction zones. The same principle is adopted to bond the IPE to the passing-through plates.

Regarding the boundary conditions, the hinges are modelled by suppressing the corresponding degrees of freedom to all nodes at both column end-sections. The cantilever beams have been restrained laterally from each side of the column in order to prevent lateral torsional buckling. Simulations are performed in a displacement-controlled manner, acting on beam edges on both sides located at 2.5 m distance from column axis.

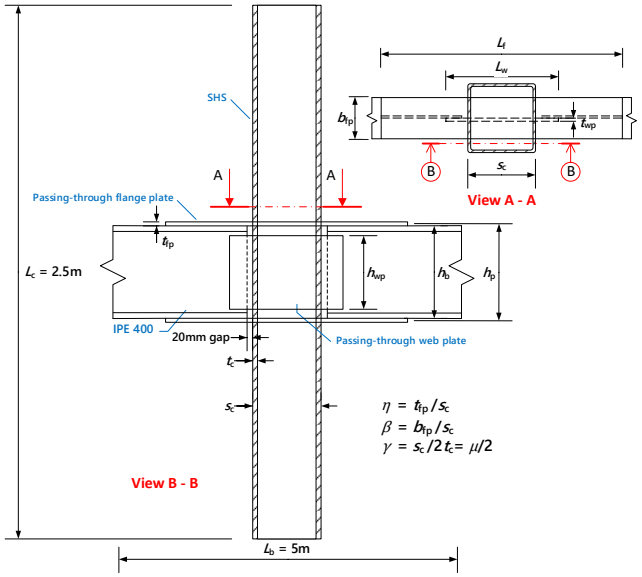

Figure 2 Joints geometric parameters

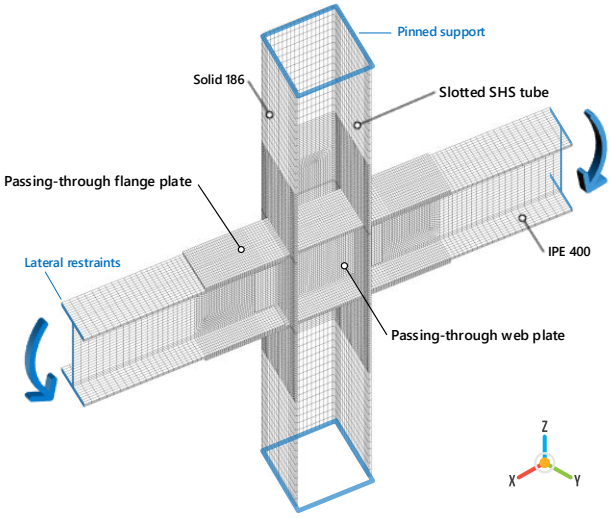

Figure 3 General mesh layout and boundary conditions

Before performing a non-linear analysis, a linear static simulation is launched first, followed by a linear buckling analysis. An imperfection homothetic to the buckling modes corresponding to passing-through plates buckling has been introduced. The imperfection is equal to s_c /200 according to Table 5.1 of Eurocode 3 part 1-1 [11].

2.3 Primary investigation

In this section, the behaviour of a SHS350x10 column crossed by flange and web passing plates of 10 and 8 mm thickness respectively is compared to an experimental test [6] performed on a CHS355.6x10 column instead of a SHS350x10.

Under equal hogging bending moments, failure is due to the development of plastic hinges in the compressed passing through plate portion inside the tube-wall. The bottom flange plate buckling marks the peak of the joint behaviour, followed by the web plate buckling. The post-peak behaviour is mainly influenced by the tube wall yielding. Once local buckling takes place in the passing plates, the proportion of transverse force transmitted to the tube-wall

increases. The transverse stiffness of SHS being lower than a CHS (due to the absence of arch stiffening effect), the post-buckling is characterised by a smooth decrease of the loading (see **Figure 4**). The initial stiffness is not influenced by column cross-section shape.

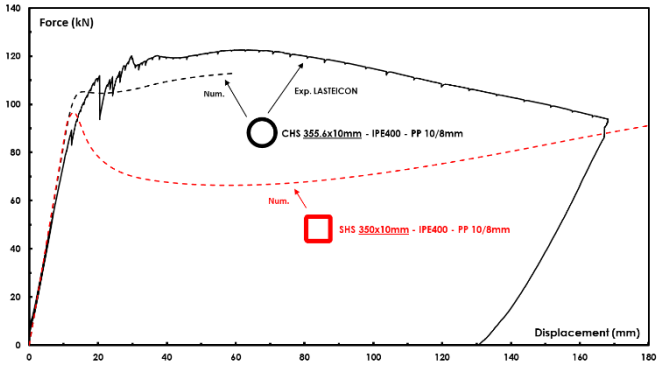

Figure 4 Comparison of joints with SHS and CHS columns

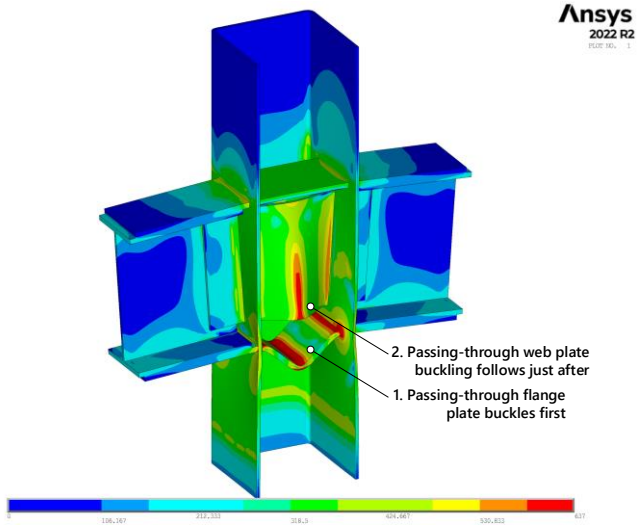

Figure 5 Typical failure mode – Von mises Stresses

2.4 Sensitivity analysis

A total of sixteen additional joints have been studied varying the column size and thickness as well as the passing though plates thicknesses. The I-beam profile corresponds to an IPE400. The flange plate width and web plate depth are equal to 180 and 320 mm, respectively. Regarding the length, the passing flange measures 970 mm and the passing web size is of 550 mm for SHS350 and 500 mm for configurations with SHS300. The investigated geometries are presented in Table 1 as well as the initial rotational stiffness of the joint and the ultimate bending moment. The rotational stiffness is assessed by extracting horizontal displacement right at the junction between the passing flanges and the tube-wall.

Table 1 Geometry details and numerical results

Geometrical parameters					Main results	
	s_c	t_c	t_f	t_w	$S_{j,ini}$	$M_{j,u,num}$
	mm	*mm*	*mm*	*mm*	*kNm*	*kNm*
SET 1	**Passing plates of 10 and 8mm thickness**					
1.1	350	10	10	8	181,0	225,0
1.2	350	12,5	10	8	193,8	237,9
1.3	300	10	10	8	220,2	259,7
1.4	300	12,5	10	8	232,6	274,5
SET 2	**Passing plates of 12 and 10mm thickness**					
2.1	350	10	12	10	226,5	313,7
2.2	350	12,5	12	10	234,2	325,4
2.3	300	10	12	10	267,7	346,9
2.4	300	12,5	12	10	280,0	363,5
SET 3	**Passing plates of 15 and 10mm thickness**					
3.1	350	10	15	10	282,8	417,2
3.2	350	12,5	15	10	290,7	429,3
3.3	300	10	15	10	334,9	451,3
3.4	300	12,5	15	10	347,1	469,6
SET 4	**Passing plates of 20 and 12mm thickness**					
4.1	350	10	20	12	368,7	553,8
4.2	350	12,5	20	12	379,4	553,4
4.3	300	10	20	12	437,3	577,3
4.4	300	12,5	20	12	452,3	588,1

The vertical load-displacement curves are depicted for sets 1 and 4 in **Figure 6.** For passing plates of 10/8, 12/10 and 15/10mm, the failure is due to passing-flange buckling followed by passing-web buckling. A clear peak load can be observed *(see* **Figure 6-a***)*. The post-peak behaviour depends on the SHS dimensions.

However, for passing plates of 20/12mm thickness, the failure starts outside the joint node, by beam flange buckling in compression, followed by passing-through flange buckling (see **Figure 6-b**). With a SHS350x10mm, the passing-through web buckled shortly after passing-through flange failure. This latter phenomenon was not observed for the rest of configurations in set 4.

Besides, what emerges from the results is that the passing through plates thicknesses have a primary role in the bending resistance of the joint. Shifting from 10/8mm to 12/10mm passing plates improved the joint resistance by 32 to 39%. The gains are more pronounced when going from 10/8mm to 15/10mm passing plates, with an enhancement of 71 to 85%. Regarding the stiffness, the increase is less significant with 8.6% among studied configurations between 10/8mm and 12/10mm passing plates.

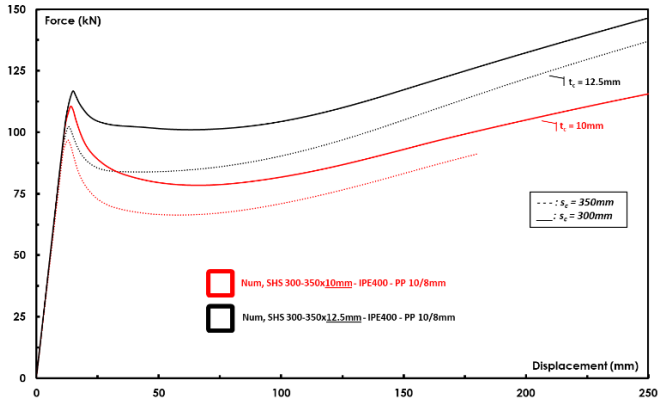

a. **Set 1:** Passing plates thicknesses at 10/8mm, and varying SHS dimensions

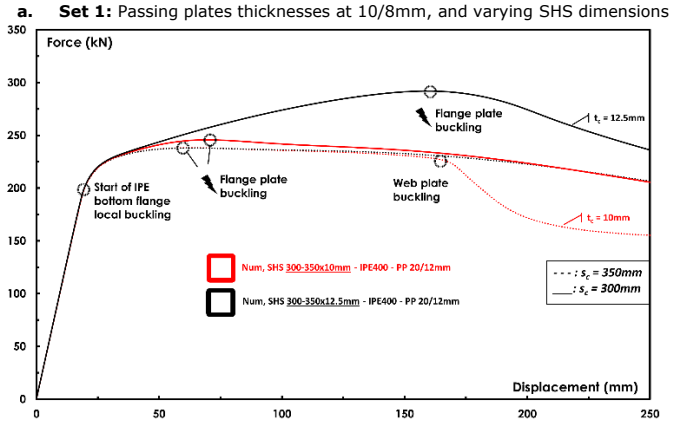

b. **Set 4:** Passing plates thicknesses at 20/12mm, and varying SHS dimensions

Figure 6 Load – deformation curves

The SHS side size also influences the joint behavior. A decrease of the tube size enhances the resistance as the buckling length decreases. The contribution of the column thickness is more limited as the tube transverse stiffness is lower comparatively to the passing-through plate's stiffness.

3 Analytical model

3.1 Bending resistance

The analytical model proposed to determine the bending resistance and initial rotational stiffness is based on assumptions similar to those suggested by Couchaux et al. [6] for joints composed of CHS column but adapted to SHS one's. The failure mode corresponds to buckling of flange plates inside the tube. The stiffness of the different components is considered for the evaluation of force distributions within the joint. The components are:

- Flange plates in compression/tension,
- Web plate in bending,
- Tube-wall in transverse tension/compression.

Using rotation compatibility and force equilibrium based on the simplified model presented in **Figure 7**, the bending resistance is:

$$M_{j,u} = \eta_t \eta_I F_{fp,I,u} h_p \quad (1)$$

Where: $\eta_t = 1 + \frac{k_t}{k_{fp}}$

And: $\eta_I = 1 + \frac{I_{wp}}{I_{fp}.\eta_t}$

Where k_{fp} is the axial stiffness of the passing-through flange. h_p is the distance between the middle lines of the passing-through flanges.

I_{wp} and I_{fp} are moments of inertia of the passing web and flange plates, respectively.

k_t corresponds to the SHS column transverse stiffness:

$$k_t = \frac{E}{\frac{1}{k_a} + \frac{1}{k_b}} \quad (2)$$

Where:

k_a: stiffness of the SHS face in bending,

k_b: stiffness of SHS side-walls in axial tension/compression.

The stiffness of the SHS in bending is calculated according to Costa-Neves semi-analytical expression, as stated in [8] by Garifullin et al:

$$k_a = \frac{t_c}{14.4\mu^2}\left(\frac{\mu}{\beta}\right)^{1.25} \cdot \frac{\mu + (1-\beta).tan(\theta)}{(1-\beta)^3 + \frac{10.4(1.5-1.6\beta)}{\mu^2}} \quad (3)$$

Angle θ is represented in **Figure 8**, and can be calculated as follows:

$$\theta = \begin{cases} 35 - 10\ b_{fp} & \text{if } = \beta < 0.7 \\ 49 - 30\ b_{fp} & \text{if } = \beta \geq 0.7 \end{cases}$$

The side-wall compression/tension stiffness is:

$$k_b = 2 \times 0.7 b_{eff} \frac{t_c}{s_c} \quad (4)$$

With t_c and s_c the thickness and side size of the SHS column.
And: $b_{eff} = t_{fp} + 5t_c$, with t_{fp} the thickness of the flange plate.

The multiplier 2 in equ.(4) accounts for both lateral walls.

The buckling resistance of the flange passing plate, $F_{fp,I,u}$, is calculated according to Eurocode 3 part 1-1:

$$F_{fp,I,u} = \chi_{fp} F_{pl} = \chi_{fp} A_{fp} f_{y,fp} \quad (5)$$

With χ_{fp} the reduction factor for relevant buckling curve. $f_{y,fp}$ corresponds to the flange plate yield strength and A_{fp} is its area.

Here, the calculation was performed with respect to imperfection curve "c" according to EC3 part 1-1 requirements for a solid rectangular section.

The plate is assumed clamped at both edges; the effective buckling length is thus:

$$L_{cr,eff} = \frac{s_c - t_c}{2} \quad (6)$$

The Euler elastic critical buckling load is finally:

$$F_{fp,cr} = \frac{\pi^2 E I_{fp,z}}{L_{cr,eff}^2} \quad (7)$$

Below, intermediary needed parameters are:

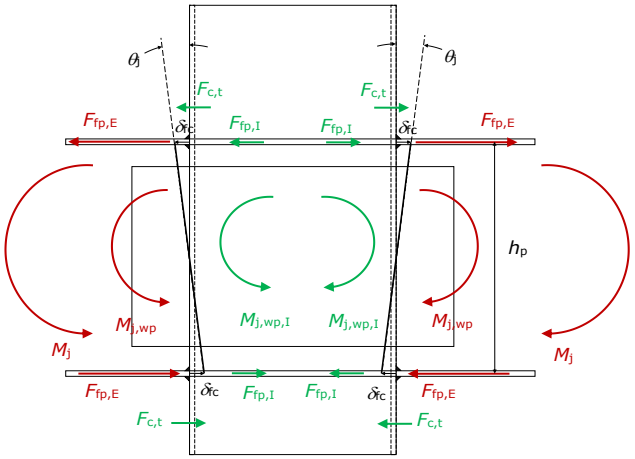

a. Forces transmission

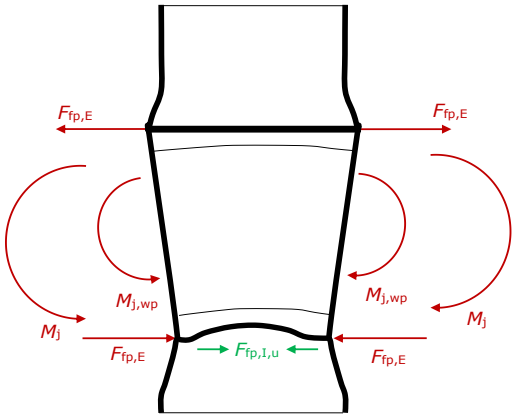

b. Failure mechanism

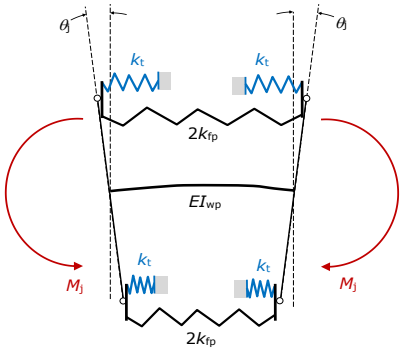

c. Spring model

Figure 7 Simplified mechanical model

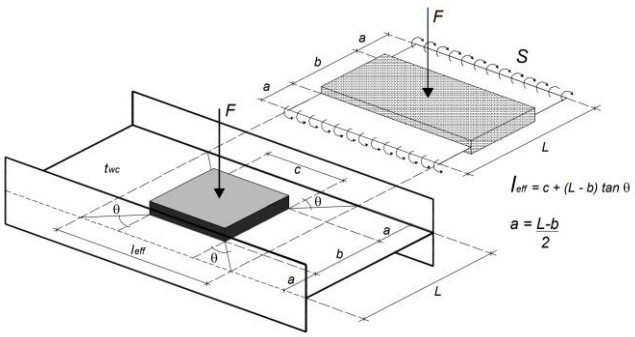

Figure 8 Strip model – Neves et al. [9]

$$\chi_{fp} = \frac{1}{\phi_{fp} + \sqrt{\phi_{fp}^2 - \bar{\lambda}_{fp}^2}}$$

$$\bar{\lambda}_{fp} = \sqrt{\frac{A_{fp} f_{y,fp}}{F_{fp,cr}}}$$

$$\alpha_{fp} = 0,49$$

$$\phi_{fp} = 0,5\left(1 + \alpha_{fp}(\bar{\lambda}_{fp}^2 - 0,2) + \bar{\lambda}_{fp}^2\right)$$

3.2 Initial rotational Stiffness

Based on the spring model represented in Figure 7-c, and by equating the rotation of the passing plates and the tube face at junction, the initial rotational stiffness can be expressed as:

$$S_{j,ini} = \frac{\eta_t \eta_1 k_{fp} h_p^2}{2} \quad (8)$$

Where the lever arm equals:

$$h_p = h_b + t_{fp} \quad (9)$$

With h_b the height of the I-beam and t_{fp} the thickness of the passing flange plate.

Moreover, the initial rotational stiffness can be re-written in a better convenient form:

$$S_{j,ini} = \left(k_{fp} + k_t\right) h_p^2 / 2 + S_{j,wp} \quad (10)$$

With $S_{j,wp}$ the bending stiffness of the passing-web plate.

4 Comparison to numerical results

The bending resistance and initial rotational stiffness calculated analytically and numerically are presented in **Table 2**. The results are in good agreement particularly concerning the bending resistance with a mean value of 0,98 and a standard deviation of 4%. The analytical model is able to capture the beneficial effects of increase of passing plate and tube thickness's as well as the decrease of SHS side. The precision concerning the initial rotational decrease with a mean value of 1,12 but the results are satisfactory.

Table 2 Comparison of numerical and analytical results

	$M_{j,u,num}$	$M_{j,u,ana}$	-	$S_{j,ini,num}$	$S_{j,ini,ana}$	--
	kNm			*kNm/mrad*		
SET 1	**Passing plates of 10 and 8mm thickness**					
1.1	225,0	228,1	1,01	181,0	212,2	1,17
1.2	237,9	241,5	1,02	193,8	214,2	1,11
1.3	259,7	251,2	0,97	220,2	248,2	1,13
1.4	274,5	265,8	0,97	232,6	250,6	1,08
SET 2	**Passing plates of 12 and 10mm thickness**					
2.1	313,7	302,2	0,96	226,5	257,4	1,14
2.2	325,4	317,2	0,97	234,2	259,4	1,11
2.3	346,9	323,9	0,93	267,7	300,9	1,12
2.4	363,5	339,8	0,93	280,0	303,4	1,08
SET 3	**Passing plates of 15 and 10mm thickness**					
3.1	417,2	399,7	0,96	282,8	316,6	1,12
3.2	429,3	416,3	0,97	290,7	318,7	1,10
3.3	451,3	419,2	0,93	334,9	370,1	1,11
3.4	469,6	436,5	0,93	347,1	372,7	1,07
SET 4	**Passing plates of 20 and 12mm thickness**					
4.1	553,8	566,0	1,02	368,7	425,5	1,15
4.2	553,4	584,5	1,06	379,4	427,8	1,13
4.3	577,3	584,1	1,01	437,3	497,3	1,14
4.4	588,1*	603,2	1,03	452,3	500,2	1,11
		Mean	0,98		**Mean**	1,12
		St. Dev	0,04		**St. Dev**	0,03

*Bending moment evaluated at the beam local buckling section.

5 Conclusions

The present paper summarises the numerical and analytical investigations performed on the behaviour of I-beam-to-SHS column moment resisting joints using passing-through under equal bending moments. Passing-through plates to SHS-column full joint has been studied using 20-nodes SOLID186 elements in ANSYS under gravitational loading. Connection numerical strength capacity and initial stiffness were then compared to experimental test results from LASTEICON project and analytical predictions from current literature.

The comparison between CHS and SHS profiles shows that the global behaviour is similar for both section shapes. The failure mode remains unchanged and is governed by the buckling of both, the passing-flange in compression and the passing-through web in bending. However, the post-buckling behaviour is different between SHS and CHS as a consequence of a different flexibility in bending. The parametric study highlighted that the **passing through plates thicknesses** play a **primary role** in determining both the resistance and stiffness of the assembly. Increasing the flange plate thickness to 20 mm allowed to observe the failure on the beam. Varying tube geometry also contributes to connection strength but have no clear impact on joint stiffness. As a matter of fact, the side size directly interferes with the failure mechanism since it influences the buckling length of the passing-plates. A thicker column also means that fewer forces are transmitted to the internal portion of the passing-plates. Finally, the comparison of the analytical model predictions against numerical results leads to satisfactory strength and stiffness matchings.

The proposed analytical and numerical models should be validated by comparison to experimental tests.

References

[1] Packer, J. (1978) *A theoretical analysis of welded steel joints in rectangular hollow sections* [PhD Thesis]. University of Nottingham.

[2] EU-RFCS project LASTEICON 709807 (2016-2020) lasteicon.eu

[3] Schneider, S.P.; Alostaz, Y.M. (1998) *Experimental Behavior of Connections to Concrete-Filled Steel Tubes.* Journal of Constructional Steel Research, Vol.45, Issue 3, p.321-352.

[4] Alostaz, Y.M.; Schneider S.P. (1996) *Analytical behavior of connections to concrete-filled steel tubes*. Journal of Constructional Steel research, Vol.40, p.95–127.

[5] EU-RFCS project LASTTS 101034038 (2021-2024) lastts.eu

[6] Couchaux, M.; Castiglioni, C.A.; Hjiaj, M.; Wald, F. (2021) *I-beam-to-CHS-column moment resisting joints using passing-through plates*. Journal of Constructional Steel Research, Volume 184, 106703.

[7] Das, R.; Kanyilmaz, A.; Couchaux, M.; Hoffmeister, B.; and Degee, H. (2020) *Characterization of moment resisting I-beam to circular hollow section column connections resorting to passing-through plates*. Engineering Structures, Volume 210, 110356.

[8] Garifullin, M.; Pajunen, S.; Mela, K.; and Heinisuo, M. (2018) *3D component methos for welded tubular T joints*. 16th ISTS, Melbourne Australia, 2017.

[9] Neves, L. C.; da Silva, L. S.; and Vellasco, P. C. G. S. (2005) *A model for predicting the stiffness of beam to concrete filled column and minor axis joints under static monotonic loading*. Eurosteel, Université de Liège und Rheinisch-Westfälische Technische Hochschule Aachen, 2005.

[10] Packer, J.A.; Wardernier, J.; Zhao, X.L.; Van der Vegte and Kurobane, Y. (2009) *Design guide for rectangular hollow section (RHS) joints under predominantly static loading*. Cidect, Second Edition.

[11] CEN Eurocode 3 (2005) – *Design of steel structures. Part 1-1: General rules and rules for buildings*.

ORIGINAL ARTICLE

I-beam-to-SHS column moment resisting joints using passing-through plates under opposite bending moments: numerical and analytical studies

Mouad MADHOUNI[1] | Maël COUCHAUX[1] | Mohammed HJIAJ[1] | Alper KANYILMAZ[2]

Correspondence

M.Sc., Mouad Madhouni

Institut National des Sciences Appliquées de Rennes
20 Avenue des Buttes des coesmes
35700 Rennes

Email: mouad.madhouni@insa-rennes.fr

[1] Institut National des Sciences Appliquées, Rennes, France
[2] Politecnico di Milano, Italy

Abstract

As thin walled HSS columns are very flexible, they usually exhibit excessive deformation when resisting a bending moment or transverse loads. Adding exterior/interior diaphragms is one way to remedy the problem. Another option that can significantly increase strength and stiffness is to allow passing plates through the hollow column by means of Laser Cutting Technology (LCT). This solution was tested on CHS columns within the RFCS LASTEICON project. The first outcomes were promising. One of LASTTS new RFCS project's overarching concerns is to enlarge the range of application of the passing-through solution onto SHS columns.

The goal of this research paper is to present the behaviour of I-beam-to-SHS column moment resisting joints using passing-through plates under opposite bending moments. First, a solid-based finite element model is presented. This model is used to conduct a sensitivity analysis with different SHS column and passing plates geometry. The failure mode is resulting contribution of both weld/tube-wall tearing in tension, and chord face crushing in compression. Analytical models are developed in an attempt to ascertain the bending resistance and initial rotational stiffness of this new type of connections.

Keywords

Passing-though plates / Moment resisting joints / Laser cutting technology / Tubular structures / Column panel shear.

1 Introduction

Hollow Structural Section members feature high structural performance and aesthetic design [1]. However, bolted beam-to-hollow section column joints can be challenging to erect because of their lack of accessibility. For thin-walled tubular joints, it is often required to stiffen the zone around the connection in order to limit excessive deformation and chord yielding. Numerous stiffening schemes have been developed, and internal/external diaphragms are usually adopted. Nevertheless, the reinforcement details of these solutions are often cumbersome, likely expensive, and time-consuming. A promising alternative solution is passing-through plates, which has been studied in the RFCS project LASTEICON [2] for CHS columns and has pinpointed that the welding type influences the mechanical behaviour under seismic loading ([3], [4]). The RFCS project LASTTS [5] will enlarge the scope of this research studying SHS columns. These Hollow Sections are very popular for trusses and columns, since they allow for easy connections due to their flat faces.

Under opposite bending moments, the failure is marked by weld/tube-wall in tearing concomitantly with local plastic deformation near the crushing zones. Hence, the connection fails to exhibit a clear peak or yield load capacity. This failure has been observed experimentally [6], and numerically [7] for CHS columns.

The goal of this paper is to evaluate numerically and analytically the behaviour of I-beam-to-SHS-column joints made with passing-through plates under opposite hogging/sagging bending moments. Section 2 discusses finite element analyses. The non-linear finite element model with brick elements is thoroughly described. The behaviours of joints constructed with SHS and CHS columns are compared. In addition, a sensitivity analysis is performed to assess the influence of passing plate and column geometry on joint behaviour. Section 3 proposes an analytical model for determining the initial rotational stiffness in accordance with Benedetto's model ([8]-[10]). The bending resistance is based on the model proposed for I-beam-to-CHS-column joints using passing though plates [6].

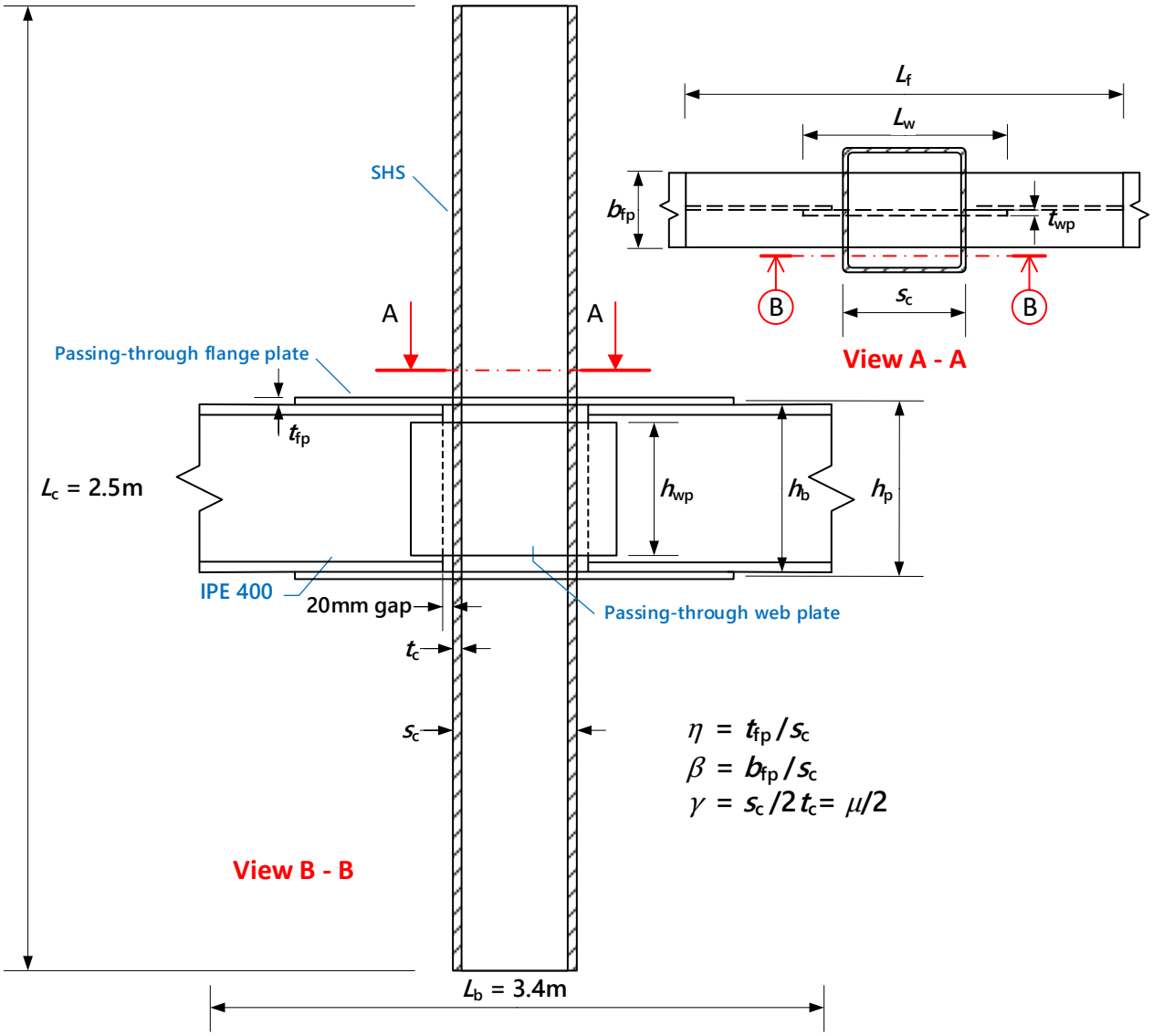

Figure 1 Joints geometric parameters

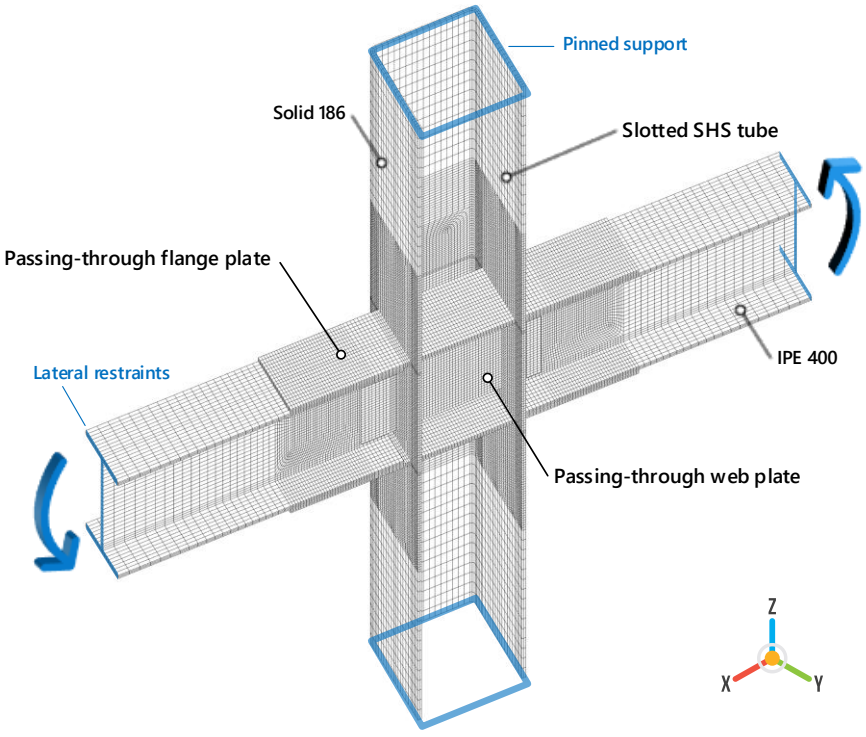

Figure 2 General mesh layout and boundary conditions

2 Finite-element model

2.1 Material properties

The mechanical properties of steel have been defined according to an elastic-plastic behaviour with kinematic hardening, adopting a Young's modulus of 210 GPa and a Poisson's ratio of 0.3. The stress-strain curve is multi-linear, based on the *true stress - true strain* curve obtained from coupon tests during LASTEICON project (see **Figure 3**). The yield stress and ultimate tensile stress are equal to 346.45 MPa and 510 MPa, respectively. The same mechanical properties have been associated to all components.

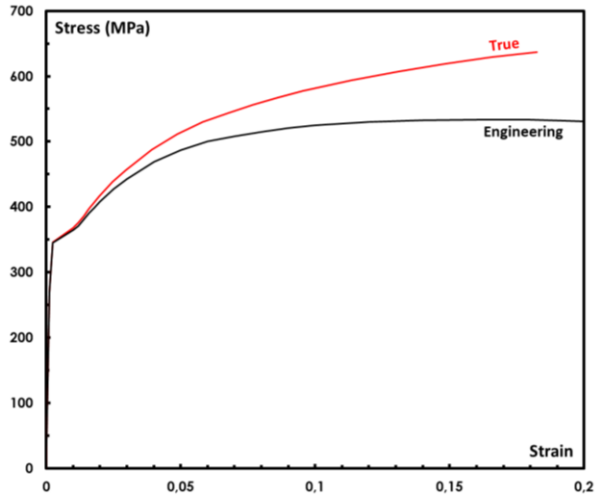

Figure 3 Steel Stress – strain curve

2.2 Joint modelling

Joints have been modelled with ANSYS 2021 R2 and analysed with non-linear static analysis. Sparse direct equation solver is used with automatic Newton-Raphson option. Furthermore, geometrical non-linearities are taken into account. 20-node solid hexahedral brick elements (SOLID186) are used. Each having three degrees of freedom per node: translations in the nodal x, y, and z directions. The general mesh layout adopts a fine mesh around the joint panel to better capture surface undulations, as well as stress and strain distributions. Moving away from the joint region, a gradual increase of element size is applied, resulting in a coarser mesh. Numerical modelling requires that at least three through-thickness elements to be used for the plates and two for the column, otherwise results may prove excessive flaw. (See **Figure 1** & **Figure 2**).

To establish a connection between the SHS column and the passing elements, the two parts share the same nodes and elements at junction zones. The same principle is adopted to bond the IPE to the passing-through plates.

Regarding the boundary conditions, the hinges are modelled by suppressing the corresponding degrees of freedom to all nodes at both column end-sections. The cantilever beams have been restrained laterally from each side of the column in order to prevent lateral torsional buckling. Simulations are performed in a displacement-controlled manner, acting on beam edges on both sides located at 1.7 m distance from the column axis.

2.3 Primary investigation

In this section, the behaviour of a SHS350x10 column crossed by flange and web passing plates of 12 and 10 mm thickness respectively is compared to an experimental test [6] performed on a CHS355.6x10 column. Under opposite hogging/sagging bending moments, the failure mechanism remains unchanged whatever the hollow section shape, and is governed by weld/tube-wall tearing in tension zones and crushing of the column faces in compression zones. Numerically, failure is marked by large strains and stresses concentration in tension and crushing zones (see **Figure 4**).

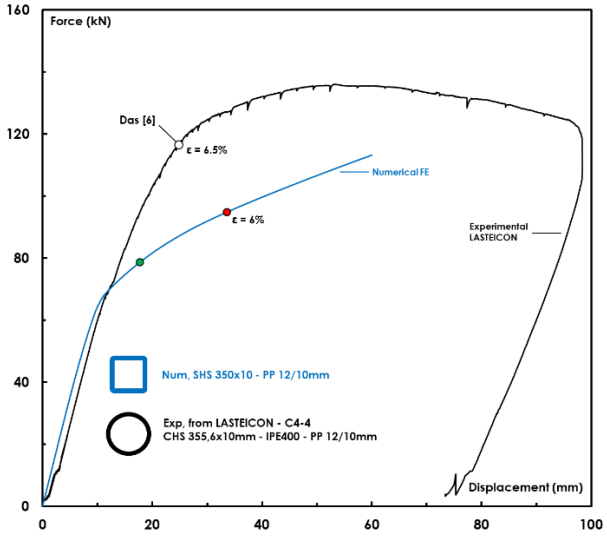

Figure 4 Comparison of joints with SHS and CHS columns

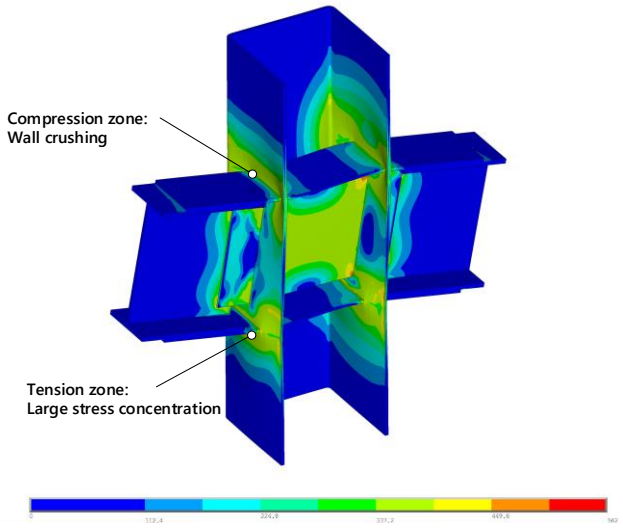

Figure 5 Typical failure mode – Von Mises stresses at 6% strain

Since damage evolution is not implemented in the FE model, the overall behaviour fails to exhibit a clear peak or yield load capacity. A strain limit criterion, equal to 6%, has been used to assess the ultimate strength and ductility of the connections (red point in **Figure 4**). To determine the yield limit, a bi-linear yield load approximation approach is adopted, in alignment with ECCS requirements n°126 (green point in **Figure 4**). The white point corresponds to the numerical resistance value [7] reported on the experimental curve from LASTEICON.

Connections using SHS prove to be more ductile and less

resistant than the one using CHS. Plastic deformation starts developing earlier for the former, resulting in a precocious loss of stiffness and higher deformation for equal strain rate compared to connections using CHS (see **Figure 4**). Since the ultimate strength is assessed using a deformation limit criterion, using SHS column rather than CHS results in lower resistance capacity.

2.4 Sensitivity analysis

A total of sixteen additional joints have been studied varying the column size and thickness as well as the passing though plates thicknesses. The I-beam profile corresponds to an IPE400. The flange plate width and web plate depth are equal to 180 and 320 mm, respectively. The passing flange length is equal to 970 mm. The passing web size is of 550 mm for SHS350 and 500 mm for configurations with SHS300. The investigated geometries are presented in **Table 1** as well as the initial rotational stiffness of the joint and the ultimate bending moment.

Table 1 Geometry details and numerical results

	Geometrical parameters					Main results	
	s_c	t_c	t_{fp}	t_{wp}	$S_{j,ini}$	$M_{j,pl,num}$	$M_{j,u,num}$
	mm	*mm*	*mm*	*mm*	*kNm*	*kNm*	*kNm*
Set1	**Passing plates of 10 and 8mm thickness**						
1.1	350	10	10	8	36,9	118,3	134,6
1.2	350	12,5	10	8	49,9	150,8	164,7
1.3	300	10	10	8	44,9	120,9	137,5
1.4	300	12,5	10	8	61,0	161,8	165,8
Set2	**Passing plates of 12 and 10mm thickness**						
2.1	350	10	12	10	45,1	134,8	139,1
2.2	350	12,5	12	10	56,3	170,5	189,7
2.3	300	10	12	10	50,5	138,4	160,2
2.4	300	12,5	12	10	67,9	180,3	189,4
Set3	**Passing plates of 15 and 10mm thickness**						
3.1	350	10	15	10	46,3	139,3	161,6
3.2	350	12,5	15	10	58,0	176,0	200,8
3.3	300	10	15	10	52,3	142,9	169,2
3.4	300	12,5	15	10	70,5	186,4	202,4
Set4	**Passing plates of 20 and 12mm thickness**						
4.1	350	10	20	12	53,0	165,1	191,6
4.2	350	12,5	20	12	65,8	202,0	233,1
4.3	300	10	20	12	59,5	167,3	198,8
4.4	300	12,5	20	12	79,8	212,3	236,6

The joint rotation is calculated with:

$$\theta_j = \theta_{num} - \frac{M_E}{S_{t,Bending}} = \theta_{num} - M_{E,num} \cdot \frac{L_c}{24.EI_c} \qquad (1)$$

With: $\theta_{num} = \frac{2\delta_{fp}}{h_p}$

δ_{fp}: Horizontal displacement at the junction between the tube and the passing flanges (see **Figure 6**).

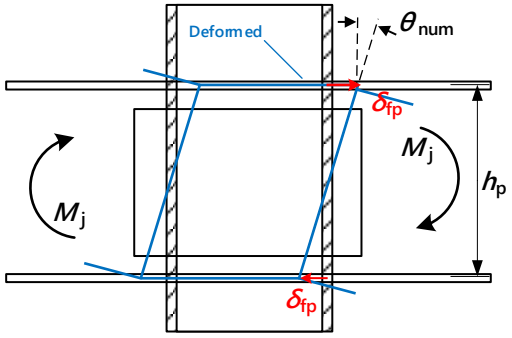

Figure 6 Evaluation of numerical rotation

The ultimate bending moment corresponds to the point at which the total equivalent Von Mises strain reaches 6% (red points in **Figure 4** and **Figure 7**).

The applied force is presented as a function of the vertical displacement in **Figure 7a** for set 2. The behaviour remains identical when looking at the rest of the understudied configurations, as demonstrated in **Figure 7b**.

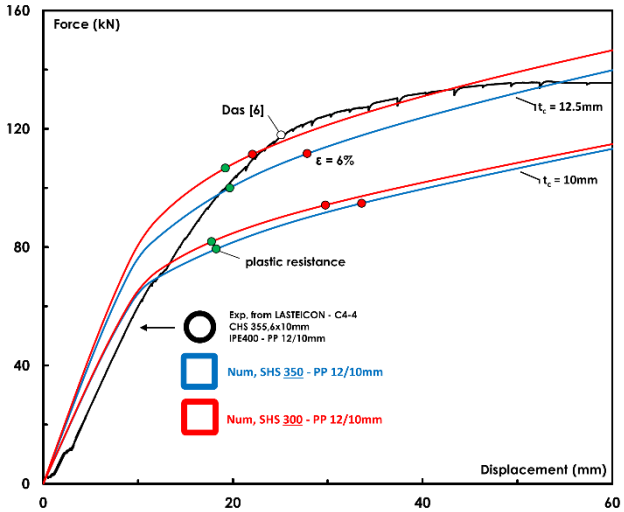

a. **Set 2:** Passing plates thicknesses at 12/10mm, and varying SHS dimensions

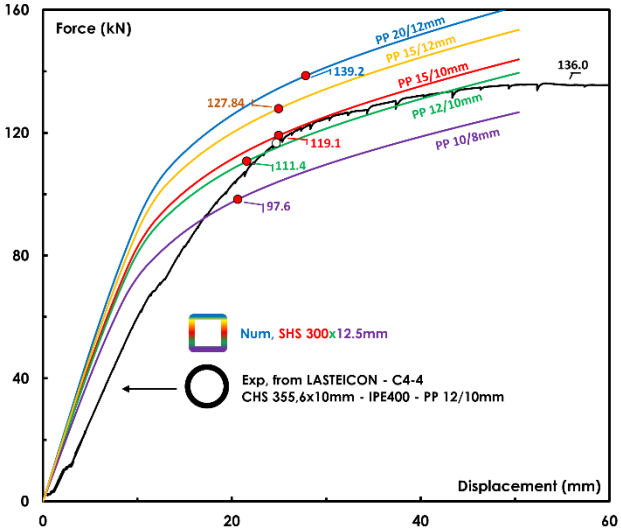

b. Varying passing plates thicknesses, and fixing SHS dimensions

Figure 7 Load – deformation curves

What emerges from the results is that the column thick-

ness plays a primary role in determining both the resistance and the stiffness of the assembly, switching from a 10mm to 12.5mm column thickness improved the joint capacity by 18 to 36%. The increase in rotational stiffness is also significant, ranging between 25% and 36% among studied configurations.

The tube side size seems to have noticeable yet limited influence on joint strength (7.3% in best case). On the other hand, gains in stiffness can be clearly observed when decreasing SHS side size (up to 22%), especially when using 12.5mm thick SHS.

Increasing passing-through plates thicknesses also has an essential role in determining both the resistance and the stiffness of the assembly. This effect is observed for all studied specimens (see **Figure 7b**). Switching from a 10/8mm to 12/10mm passing plates improved the joint capacity by 3% to 16.5% depending on the SHS dimensions. The increase in stiffness was also significant, ranging between 11.3% and 22% among studied configurations.

3 Analytical model

3.1 Bending resistance

The analytical model proposed to determine the bending resistance is adapted from Couchaux et al [6] to account for SHS columns instead of CHS. The failure mode corresponds to weld/tube fracture and is accompanied by large shear deformations of the tube. The bending resistance is mainly limited by two components:

- Tube-wall in transverse tension/compression,
- Web plate in shear.

First, the total bending moment $M_{j,u}$ is distributed between the passing flanges and web plates. Resulting in both tensile and compressive forces ($F_{fp,c,u}$ and $F_{fp,t,u}$) in the passing flanges. The second part goes through the passing-through web in bending (See **Figure 8**):

$$M_{j,u} = M_{j,fp,u} + M_{j,wp,u} \tag{2}$$

Where the bending resistance of the web plate $M_{j,wp,u}$ is:

$$M_{j,wp,u} = \frac{V_{wp,u} s_c}{2} \leq \frac{h_{wp}^2 t_{wp} f_{y,wp}}{4} \tag{3}$$

$V_{wp,u}$ is the ultimate shear capacity of the web:

$$V_{wp,u} = h_{wp} t_{wp} \frac{f_{y,wp}}{\sqrt{3}} \tag{4}$$

Where $f_{y,wp}$ is the yield strength of the web plate.

The contribution of the flange plates to the bending resistance is:

$$M_{j,fp,u} = F_{fp,u} h_c \leq V_{cp,u} h_c \tag{5}$$

The resistance of SHS column to transverse force transmitted by the passing-through flanges can be determined according to table 9.16 of prEN 1993-1-8:2020 [11].

$$F_{fp,u} = f_{y,c} t_c^2 \left(\frac{2 + 2.8\beta}{\sqrt{1 - 0.9\beta}} \right) Q_f . C_f \tag{6}$$

With Q_f the stress factor, defined according to section 9.2.1 (4) of prEN 1993-1-8 [11]. It accounts for resistance reduction due to loading. Hence, the calculation should be carried iteratively.

And C_f is the material factor to resistance equal to one, according to Table 9.1 of EN 1993-1-8 in the present case.

The force transmitted by the flange plates to the column generate a shear force on the column cross-section and will be limited by its shear resistance:

$$V_{cp,u} = 0.9 \frac{f_{y,c} A_{vc}}{\beta_V \sqrt{3}} \tag{7}$$

Where A_{vc} is the shear area of the column:

$$A_{vc} = 2 t_c (s_c - t_c) \tag{8}$$

β_V: transformation parameter equal to 2 in the case of opposite bending moments according to table 7.4 of prEN 1993-1-8 [11].

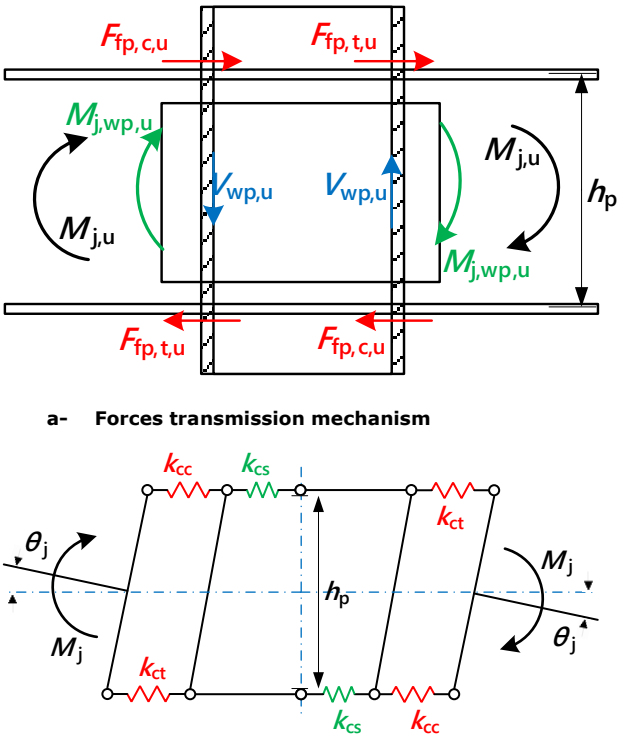

a- Forces transmission mechanism

b- Spring model

Figure 8 Simplified mechanical model

3.2 Initial rotational Stiffness

The spring model presented in **Figure 8** is based on the component method. Two components are selected:

- SHS face in tension k_{ct}, and in compression k_{cc},
- Column and web panel in shear k_{cs}.

According to Eurocode 3 Part 1-8 [11], the joint stiffness can be expressed as:

$$S_{j,ini} = \frac{Ez^2}{\sum \frac{1}{k_i}} = \frac{E\, h_p^2}{\frac{1}{k_{cs}} + \frac{2}{k_{ct}}} \quad (9)$$

The stiffness factor k_{cs} is very similar to the formulation proposed in Annex A (A.5) of prEN 1993-1-8:2020 [11] corresponding to column web panel's stiffness in shear.

$$k_{cs} = \frac{\alpha_1 . A_{v,SHS+WP}}{h_p \beta_V} \quad (10)$$

With: $\alpha_1 = \frac{1}{1.228}$ and $A_{v,SHS+WP} = 2(s_c - t_c)t_c + t_w s_c$

It is worth noting that the adopted factor slightly differs by introducing a calibration coefficient α_1 in order to account for the interaction between the two components of the panel working in shear. This coefficient substitutes the constant parameter 0,38 that corresponds to the fraction ½(1+v).

$$k_{cc} = k_{ct} = 2\alpha_2 . \frac{b_{eff} . t_c}{s_c} \quad (11)$$

Where: $\alpha_2 = \frac{1}{0.056}$ and $b_{eff} = \frac{b_{fp}}{\sqrt{1.5}}$

Both k_{cc} and k_{ct}, are defined according to Annex A (A.23) of prEN 1993-1-8:2020 [11] stiffness formulation corresponding to column web in transverse tension. An effective width b_{eff} is used in order to account for stress non-uniform distribution due to the interaction between the passing plate and the column walls. Wardenier et al. [11] developed an expression for branch plate to RHS connections, introducing a function $f(\beta)$ to account for less than full width connections (β <1). Consequently, the effective width is taken as b_{fp} / √1.5, fixing f(β) to 3,2 for the studied cases. It is to note than no clear trend for f(β) has been reported by Wardenier. Determination of this factor was examined through a "trial and error" process in comparison with the obtained numerical value.

Similar to k_{cs}, a second calibration factor α_2 is introduced. Benedetto et al. performed a parametric analysis on I-beam to CHS column one-sided joints, and provided values for the regression coefficients α_1 and α_2 [6]. Although these values were established for CHS profiles, adopting them for assessing the rotational stiffness of SHS profiles seems to lend satisfactory results.

4 Comparison to numerical results

The bending resistance and initial rotational stiffness calculated analytically are compared to numerical results in **Table 2**.

The numerical and analytical results fitly match in general. For the joint strength, the model seems to generally land values erring on the safe side, with a mean value of 0,97 and a standard deviation of 5%. Regarding the rotational stiffness, the spring model and adopted parameters give accurate predictions when compared to numerical values, except for thin passing-through plates (Set 1) in which the analytical formulation overestimates the stiffness with regards to numerical findings.

Table 2 Comparison of numerical and analytical results

	$M_{j,pl,num}$	$M_{j,u,ana}$	-	$S_{j,ini,num}$	$S_{j,ini,ana}$	--
	kNm			*kNm/mrad*		
S1	**Passing plates of 10 and 8mm thickness**					
1.1	118,29	122,7	1,04	36,9	45,8	1,24
1.2	150,81	157,8	1,05	49,9	57,3	1,15
1.3	120,88	122,1	1,01	44,9	53,3	1,19
1.4	161,85	161,3	1,00	61,0	66,6	1,09
S2	**Passing plates of 12 and 10mm thickness**					
2.1	134,76	137,4	1,02	45,1	46,3	1,03
2.2	170,46	172,5	1,01	56,3	57,8	1,03
2.3	138,42	134,6	0,97	50,5	53,9	1,07
2.4	180,28	173,7	0,96	67,9	67,3	0,99
S3	**Passing plates of 15 and 10mm thickness**					
3.1	139,32	137,8	0,99	46,3	47,0	1,01
3.2	176,00	173,2	0,98	58,0	58,7	1,01
3.3	142,94	135,0	0,94	52,3	54,7	1,05
3.4	186,37	174,5	0,94	70,5	68,3	0,97
S4	**Passing plates of 20 and 12mm thickness**					
4.1	165,07	153,0	0,93	53,0	48,1	0,91
4.2	202,98	188,6	0,93	65,8	60,1	0,91
4.3	167,31	147,9	0,88	59,5	56,0	0,94
4.4	212,26	187,6	0,88	79,8	69,9	0,88
		Mean	0,97		**Mean**	1,03
		St. Dev	0,05		**St. Dev**	0,10

5 Conclusions

The current work summarizes the numerical and analytical analyses conducted on the behaviour of I-beam-to-SHS column moment resisting joints employing passing-through plates under opposite bending moments. Passing-through plates to SHS-column full joints were investigated using 20-node SOLID186 elements in ANSYS under opposite bending moments generally produced by lateral loads (wind, seismic). The numerical results were then compared to experimental test outcomes from the LASTEICON project as well as analytical predictions from the suggested model.

The comparison between CHS and SHS profiles shows that the global behaviour is similar for both section shapes. The failure mode remains unchanged and takes place by excessive shear deformation in the column panel, and happens by welds/tube fracture in tension zones and column faces crushing in compression ones. However, yielding is reached precociously when using SHS profile compared to CHS as a consequence of a different flexibility in bending.

What emerges from the parametric study is that the column and passing plates thicknesses have a primary role in determining both the resistance, stiffness and ductility of the assembly. Varying SHS side size has a small, yet noticeable, effect on both ductility and joint strength capacity. However, significant gains in stiffness can be observed when decreasing SHS side size, especially when using thin passing-through plates.

Finally, the comparison of the analytical model predictions against numerical results leads to satisfactory strength and stiffness matchings.

Acknowledgments

This project has received funding from the European Union, Research Fund for Coal and Steel under grant agreement No 101034038.

References

[1] Packer, J. (1978) *A theoretical analysis of welded steel joints in rectangular hollow sections* [PhD Thesis]. University of Nottingham.

[2] EU-RFCS project LASTEICON 709807 (2016-2020) lasteicon.eu

[3] Schneider S.P., Alostaz Y.M. (1998) *Experimental Behaviour of Connections to Concrete- Filled Steel Tubes*, Journal of Constructional Steel Research, Vol.45, Issue 3, p.321-352.

[4] Alostaz Y.M., Schneider S.P. (1996) *Analytical behaviour of connections to concrete-filled steel tubes*, Journal of Constructional Steel research, Vol.40, p.95–127.

[5] EU-RFCS project LASTTS 101034038 (2021-2024) lastts.eu

[6] Couchaux M., Castiglioni C.A., Hjiaj M., Wald F. (2021) *I-beam-to-CHS-column moment resisting joints using passing-through plates*, J. Construct. Steel Research, Volume 184, 106703.

[7] Das R., Kanyilmaz A., Couchaux M., Hoffmeister B., Degee H. (2020) *Characterization of moment resisting I-beam to circular hollow section column connections resorting to passing-through plates*, Engineering Structures, Volume 169, 106015.

[8] S. Di Benedetto, M. Latour and G. Rizzano (2020) *Assessment of the stiffness of 3D cut welded connections with CHS columns and through I-BEAMS*, Structures, 27, p.247-258.

[9] S. Di Benedetto, M. Latour and G. Rizzano (2020) *Stiffness Prediction of Connections between CHS Tubes and Externally Welded I-Beams: FE Analyses and Analytical Study*, Materials, 13, 3030.

[10] S. Di Benedetto, M. Latour and G. Rizzano (2022) *Theoretical and experimental analysis about the stiffness of 3D cut welded connections with CHS and through I-beams.* AISC – ECCS Workshop on connections in Steel Structures, Coimbra.

[11] CEN prEN 1993-1-8 (2020) – *Eurocode 3: Design of steel structures – Design of joints*.

[12] Wardenier J., Davies G. and Stolle P. (1981). *The effective width of branch plate to RHS chord connections in cross joints.* Stevin Laboratory report No. 6-81-6, Delft University of technology.

ORIGINAL ARTICLE

Innovative One-way Connections between I-beams and CHS columns

Rajarshi Das[1] | Alper Kanyilmaz[2] | Mouad Madhouni[3] | Herve Degee[4]

Correspondence

Dr. Rajarshi Das
Hasselt University
Construction Engineering Research Group
Kantoor ACB² 1.4
Applicatiecentrum beton en bouw,
Wetenschapspark 34,
3590 Diepenbeek, Belgium
Email: rajarshi.das@uhasselt.be

[1,4] Construction Engineering Research Group, Hasselt University, Dieoenbeek, Belgium
[2] Department of Architecture, Built Environment and Construction Engineering, Politecnico di Milano, Milan, Italy
[3] INSA Rennes, Rennes, France

Abstract

Although stiffeners and gusset plates are often used in conventional I-beam-to-CHS-column connections for an efficient load transfer, they usually result in high welding quantities. Directly welding the beams to the column exposes the beams to premature flange fractures and the columns to severe local distortions. Both approaches therefore hinder the use of such connections in the industry. However, if designed efficiently, the CHS connections can offer a viable solution with an excellent structural behavior in tension, compression and bending in all directions. In this context, the present contribution proposes two new moment resisting one-way connection configurations with I-beams or steel plates passing through the CHS column, developed within the European research project LASTTS, with the aim of simplifying the fabrication process and increasing the structural performance of such joints with an effective reduction of the foretold drawbacks. The "passing-through" system is developed using a laser cut & weld technology and avoids the localized damages, premature flange failures as well as the excessive usage of stiffening plates required by the conventional CHS connections. These connections are first designed based on a recently developed code-like procedure and are then assessed through nonlinear finite element models - primarily calibrated on experimental results to validate the modelling assumptions – in order to characterize the influence of the different parameters of the joints.

Keywords

Open-to-CHS column connection, Tubular structures, Hollow section joints, Passing-through joints, Laser cut joints

1 Introduction

Very good resistance against high axial forces and bending in all directions [1], lightweight structures [2], lesser requirement of fire protection materials [3] and excellent aesthetics have emphasized upon the encouraging potential offered by CHS columns and their advantages compared to equivalent H-sections. They have also proved to be the best shape for elements under wind-, water- or wave-loading scenarios [4]. Additionally, as filling the hollow sections with concrete provides a simple way to achieve a composite behaviour (and adds strength and stiffness), it also offers an extra advantage towards fire resistance. Therefore, over the past few decades, researches have tried to implement such hollow sections in structures to improve their overall resistance by exploiting the significant advantages in offer. Several different types of open-to-hollow section joints have been developed in the current industry and CIDECT has provided significant understanding [5] regarding their strength, fire protection, wind loading, composite construction and their static and fatigue behaviour based on successful identification of the force-transfer mechanism. The current Eurocode rules regarding their design and practical implementation of such structural hollow section connections are largely based on the foretold CIDECT research works. However, in today's construction industry, the I-beam-to-CHS column connections are constructed either by directly welding the beams to the CHS column wall or by using diaphragm connections (both referred to as "conventional CHS connections" in this contribution). While in the first technique, concentrated stresses develop on the CHS wall leading to its local distortions, the second technique demands a substantial number of gusset plates and/or stiffeners, which have unfortunately limited their preference from a designer's perspective. The complex detailing requirements of these joints are noticed to compromise around 1/4th of the total structural weight, increase constructional expenses and slow down the fabrication process. Several studies have suggested that the additional stiffeners and gusset plates can cause both economic as well as practical difficulties [6] during the fabrication process and can also spoil the aesthetics. They have also shown significant vulnerability towards extreme loads such as fatigue or seismic loading

scenarios due to large stress concentrations at the open-to-CHS connection zones and high residual stresses at the welds [7]. In order to improve the behaviour of such I-beam-to-CHS connections, an innovative concept was proposed in the EU-RFCS research project – "LASTEICON" (RFCS-GA-709807) [8] where several "passing-through" connections were investigated with the primary aim to reduce or possibly avoid the local distortions and premature flange fractures occurring in the conventional open-to-CHS joints with a reduced welding quantity. The basic concept behind the LASTEICON joints are shown in Fig. 1 (with 4-way connections). All the LASTEICON connections consisted of "main" (primary) beams connected to the CHS column via one or multiple "through" elements (I-beam stub or individual steel plates) passing through laser-cut slots on the CHS column. Thanks to the several structural and economic advantages obtained from the experimental and numerical research investigations, the LASTEICON "passing-through" connections proved to be a viable alternative and was therefore extended to a new European research project – "LASTTS" [9], where novel, specialised, more complex joints have been proposed for research.

Figure 1 Laser cutting techniques, machine and approach to develop the LASTEICON and LASTTS joints. [9]

Different types of two-way and four-way "passing-through" I-beam-to-CHS joints were comprehensively investigated in the LASTEICON project [8], but due to specific requirements of some structures, an "Edge" joint configuration (Fig. 2) was deemed to be also important from an industrial perspective. To that purpose, this article presents two types of one-way moment resisting I-beam-to-CHS column connections with the "passing-through" solution. Numerical parametric studies are discussed to note the influence of the various joint parameters with relevant conclusions.

2 LASTTS one-way joint configurations

2.1 Types of Configurations

Following the basic concept behind the LASTEICON and LASTTS "passing-through" joints stated above, two types of one-way moment resisting connection configurations were investigated:

a) Configuration C1: Constituting of a "main" I-beam connected to an I-beam passing through the CHS (Fig. 2a).

b) Configuration C2: Consisting of a "main" I-beam connected to two flange plates and a web plate passing through the CHS column (Fig. 2b).

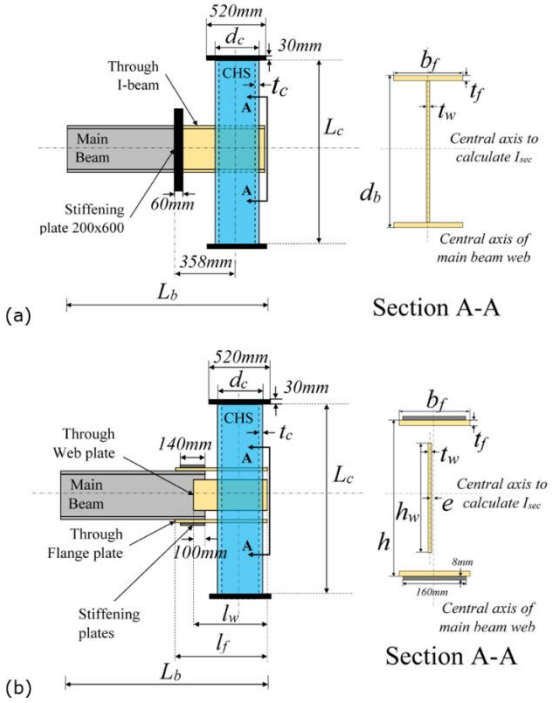

Figure 2 Schematic diagrams of LASTTS configurations (a) C1 (b) C2.

2.2 Modelling approach and boundary conditions

The configurations were modelled using 3D geometries and solid elements such as CHX60, CTP45 and CTE30 in the commercial software DIANA 10.2 [10]. The laser-cut slots on the tube surface were considered to position the through-elements and account for the necessary reduction in the tube stiffness. Circular end-plates were used at the top and bottom of the tubes during the previous LASTEICON tests and were consequently incorporated in the FE models to apply the necessary boundary conditions - translations were fixed in all directions. Both configurations were investigated through a single loading scenario (nonlinear static analysis) – applying a vertical load at the end of the main beam. This vertical load was incremented step by step from 0 till failure of the numerical model. To define "failure" in the models, a limiting value = 5% was assumed for the equivalent plastic strain –, based on previous calibration from the LASTEICON studies on 2-way joints. A S355 steel material was adopted for all structural components with elastic perfectly plastic properties without hardening. Specific assumptions were made to avoid heavy, complicated models during the preliminary investigations and also to avoid any secondary connection failure and rather focus on the "passing-through" zone:

i. The laser cut slots in the FE models were defined assuming a zero tolerance, thus connecting the tube and the passing-through elements as a perfectly welded connection.
ii. The welds were not modelled explicitly. Members were connected through common nodes.
iii. Although in reality bolts are used to realise the moment resisting connection between the main beam and the through members, perfectly welded plates were used in the FE models.

The FE models were validated based on the experimental

results obtained from the LASTEICON research investigations [11]. Although the one-way connections have not yet been tested, the FE modelling approach adopted for these joints were similar to the two-way joints studied in the LASTEICON project. Detailed results regarding the model validation can be found in the LASTEICON project report [8] for different types of joint configurations.

3 Results and discussions

3.1 Configuration C1

The through I-beam section (IPE), the CHS column thickness (t_c) and diameter (d_c), the moment-to-shear ratio (M/V) by changing the main beam length (L_b) are the four parameters varied to understand the behaviour of the C1 configuration. The maximum Von mises equivalent plastic strains and stresses are depicted for the maximum load attained in the numerical simulations. In order to understand the influence of each parameter, the different models were compared with a reference configuration with the following geometric parameters – an IPE 400 as the through I-beam, a CHS column thickness = 10 mm, diameter = 355.6 mm, and the beam length = 1.5 m. The length of the through I-beam was kept constant (= 800 mm). The reference configuration is plotted as the solid green line in all the plots presented in this section.

3.1.1 Variation of the through I-beam section (IPE)

5 different sections were used for the through I-beam: IPE 220, IPE 270, IPE 330, IPE 400 and IPE 500. The other parameters were kept constant throughout the variations. Fig. 3 shows the vertical force-displacement curves obtained from the numerical models with different through I-beam sections. The curves show that the resistance increases with a larger through I-beam section. The failure modes corresponding to the case studies with the four smaller sections were qualitatively similar. The models having through sections IPE 220, IPE 270 and IPE 400 had a flexural failure of the upper and lower flanges just outside the CHS (see Fig. 11) - this failure mode was obtained from most of the case studies described in section 3.1. However, a significant difference was noticed for the IPE 500 through beam connection as the failure occurred in the main beam rather that the through beam, indicating that the connection is stronger than the main beam itself.

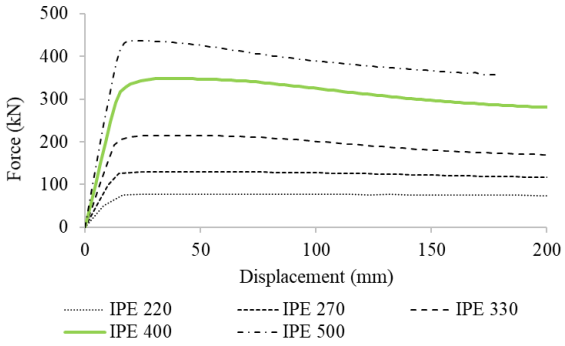

Figure 3 Vertical force-displacement curves for varying through I-beam sections (C1)

3.1.2 Variation of the CHS column thickness (t_c)

The CHS column thickness was varied from a thickness of 4 mm to 6 mm, 8mm, 10 mm and 12 mm. The vertical force-displacement curves are compared in Fig. 4. At the first glance, it can be concluded that increasing the thickness of the tube increases the resistance of the joint. The force-displacement behaviour as well as the failure modes are noticed to be reasonably similar for the case studies with CHS thicknesses = 8 mm, 10 mm and 12.5 mm - a bending failure of the I-beam flanges outside the CHS column (see Fig. 11). High shear stresses were also noticed in the web of the passing through I-beam (see Fig. 14). However, the 4 mm and 6 mm thick CHS models showcased a different behaviour. A shear failure occurred in the web of the passing-through I-beam inside the CHS column along with stress concentration on the tube wall at its connection zone with the passing through I-beam (see Fig. 5) prior to a bending failure of the I-beam flanges outside the CHS. Nevertheless, these configurations were still able to offer a ductile response as observed from the force-displacement curves in Fig. 4.

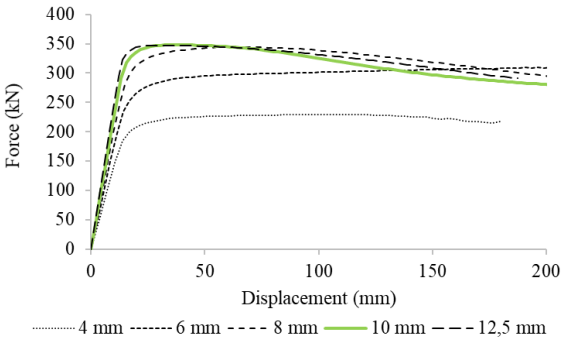

Figure 4 Vertical force-displacement curves for varying CHS column thickness (C1)

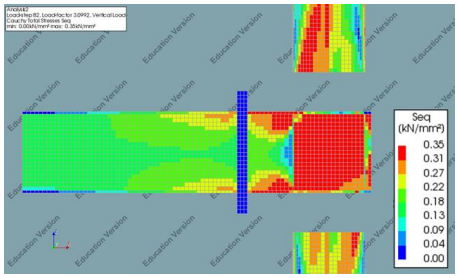

Figure 5 Von mises stresses in the models having a CHS column thickness of 4 mm and 6 mm (C1)

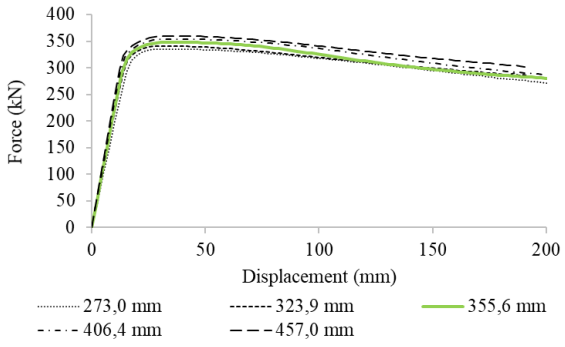

Figure 6 Vertical force-displacement curves for varying CHS column diameter (C1)

3.1.3 Variation of the CHS column diameter (d_c)

The CHS column diameter was varied from 273 mm, 323.9

mm, 355.6 mm, 406.4 mm to 457 mm. Fig. 6 compares the vertical force-displacement curves. As seen from Fig. 6, the CHS diameter does not offer a significant influence on the joint behaviour. Failure was obtained in the flanges outside the CHS column in all cases due to bending.

3.1.4 Variation of moment-to-shear (M/V) ratio

The joints were also investigated by varying the moment-to-shear (M/V) ratio at the central "passing-through" zone by varying the main beam length (L_b) from a length of 1 m to a length of 3 m (0.5 m interval). The moment-rotation curves were plotted in this case instead of the force-displacement curves as shown in Fig. 7.

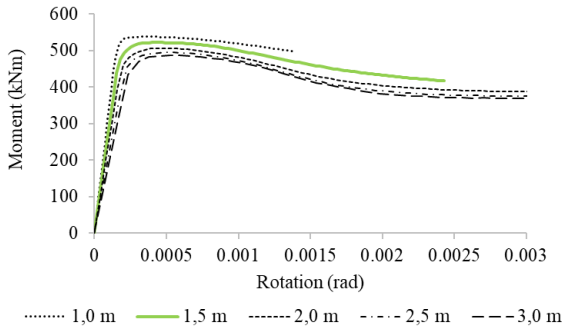

Figure 7 Moment-rotation curves for varying M/V ratio (C1)

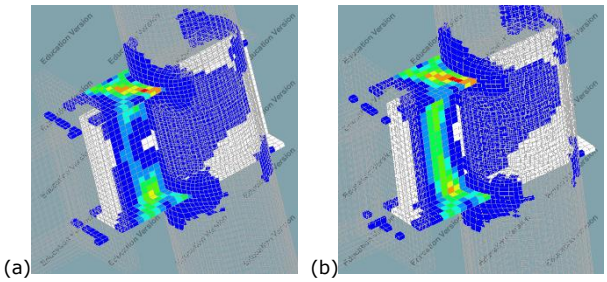

Figure 8 Equivalent plastic strains in the models having a beam length of (a) 1,5 m and (b) 2 m (C1)

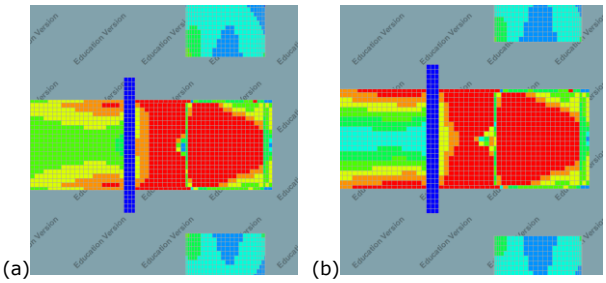

Figure 9 Von mises stresses in the models having a beam length of (a) 1,5 m and (b) 2 m (C1)

As seen from the curves, the influence of shear on the joints was found to be negligible as the moment resistance values were approximately equal for the different lengths of the beam. However, the models with a shorter beam length offered slightly higher resistance than the longer ones. This might be due to the fact that, the bending failure of the flanges (of the passing through I-beam) dominates the joint behaviour and occurs prior to a shear failure of the web. This aspect will be studied into more details after the corresponding experiments. Similar failure modes were obtained in all cases – in the flanges outside the CHS column due to bending. The equivalent plastic strains are shown in Fig. 8 and the Von mises stresses are shown in Fig. 9 for two case studies (models with a 1.5 m and 2 m long beam). High shear stresses were also noticed in the web of the passing through I-beam (Fig. 9).

3.2 Configuration C2

The "through" -flange plate thickness (t_f), the "through" -web plate thickness (t_w), the CHS column thickness (t_c) and diameter (d_c) are the four parameters varied to understand the behaviour of the C2 configuration. The maximum equivalent plastic strains and Von mises stresses are depicted for the maximum load attained during the numerical simulations. As mentioned in the previous section, the different models were compared with a reference configuration with the following geometric parameters: through flange plates of 20 mm thickness, through web plate of 10 mm thickness, CHS column thickness of 10 mm and diameter of 355.6 mm, and a beam length of 1.5 m. It corresponds to the blue solid line shown in all the plots in this section.

3.2.1 Variation of the through flange plate thickness (t_f)

The through flange plate thickness was varied from 12 mm to 20 mm (2 mm interval). Fig. 10 shows the vertical force-displacement curves for the different case studies. The curves clearly indicate that increasing the through flange plate thickness increases the resistance of the joint.

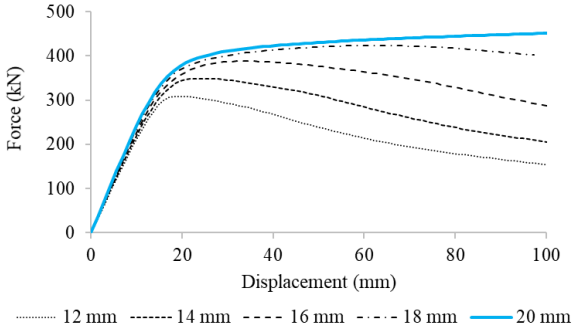

Figure 10 Vertical force-displacement curves for varying flange plate thickness (C2)

Upon observing the stresses and strains of the different case studies, a combination of failure was observed for the thinner flange plates (12 mm, 14 mm and 16 mm): bending failure of the through flange plates and shear failure of the through web plate at the connection zone just outside the CHS column (Fig. 11). Whereas, for the thicker flange plates (18 mm and 20 mm), failure occurred due to tearing of the CHS column surface at its connection with the upper flange plate at the front and the lower flange plate at the back of the tube due to tensile stresses (Fig. 15).

3.2.2 Variation of the through web plate thickness (t_w)

The through web plate thickness was varied from 10 mm to 18 mm (2 mm interval). The force-displacement curves corresponding to the web plate thickness variation are shown in Fig. 12. As shown by the curves, increasing the through web plate thickness increases the joint resistance. However, it can be said that the through web plate has a smaller influence on the joint resistance than the through

flange plates. A similar failure mode was observed for all the models: a tensile failure of the CHS column surface at its connection with the upper flange plate at the front face of the tube and its connection with the lower flange plate at the back face of the tube (see Fig. 15).

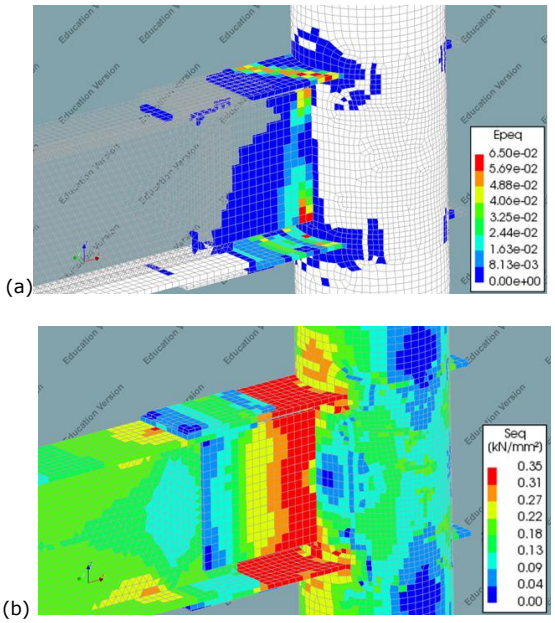

Figure 11 (a) Equivalent plastic strains and (b) Von mises stresses in the models having flange plate thickness 12 mm, 14 mm and 16 mm (C2)

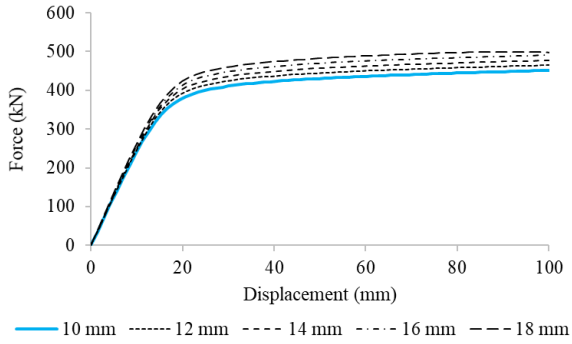

Figure 12 Vertical force-displacement curves for varying web plate thickness (C2)

3.2.3 *Variation of the CHS column thickness (t_c)*

The CHS column thickness was varied from a thinnest column of 4 mm to a thickest column of 12 mm (2 mm interval). The force-displacement curves obtained from the variation of the CHS column thickness are plotted in Fig. 13. The curves show that the joint resistance increases with increasing the thickness of the CHS column.

Although similar results were obtained for the 4 mm – 10 mm thick tubular joints, the force-displacement curve for the 12 mm thick CHS column showed a possible difference as compared to the other curves. The curve corresponding to the 12 mm thick tube bends down earlier compared to the other curves. Detailed examination of the models showed that the failure in the 12 mm thick tube model was influenced by a high stress concentration at the flanges of the main beam, which proved to be slightly weaker than the joint itself. The other models failed due to a tensile failure of the CHS column surface at its connection zone with the upper flange plate at the front face and the lower flange plate at the back face of the CHS column. High shear stresses were also noticed in the passing through web plates at the connection zone but they did not fail. Nevertheless, Fig. 15 shows the equivalent plastic strains in the CHS column highlighting the tensile failure of the CHS column surface for the other case studies with thinner tubes. Plastic strains above 5% could be observed at the tube's connection zone in the foretold locations.

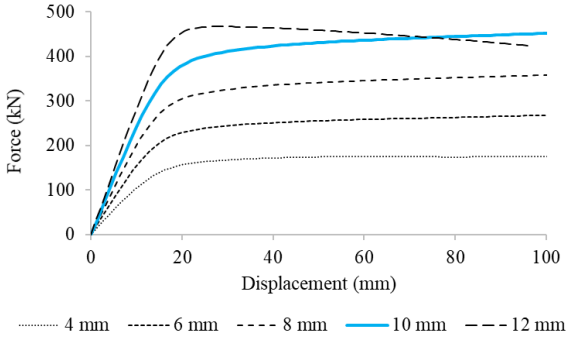

Figure 13 Vertical force-displacement curves for varying CHS column thickness (C2)

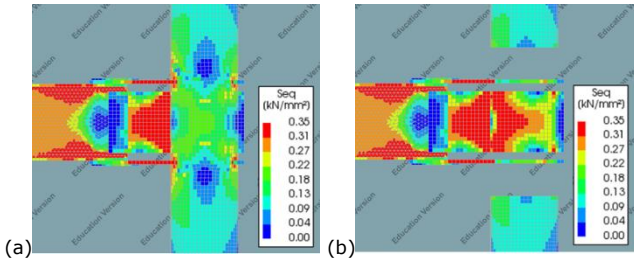

Figure 14 Von mises stresses in the model having a 12 mm thick CHS column (a) on the outer surface and (b) inside the CHS column (C2)

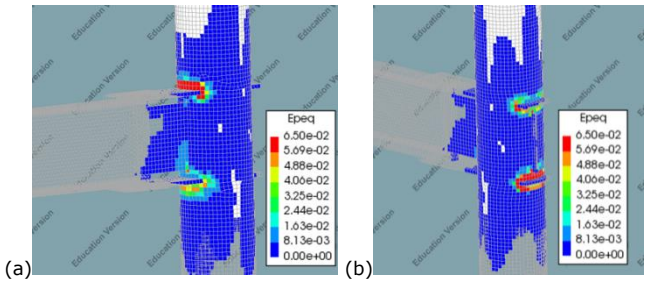

Figure 15 Equivalent plastic strains in the model having CHS column thicknesses of 4, 6, 8 and 10 mm (a) front view and (b) back view of the joint (C2)

3.2.4 *Variation of the CHS column diameter (d_c)*

The CHS column diameter was varied from 273 mm, 323.9 mm, 355.6 mm, 375 mm to 406.4 mm. The force-displacement curves obtained from the diameter variation of the CHS column are presented in Fig. 16. All cases showcased similar force-displacement behaviour as well as failure modes – a tensile failure of the CHS column surface at its connection with the upper flange plate at the front face and with the lower flange plate at the back face of the CHS column.

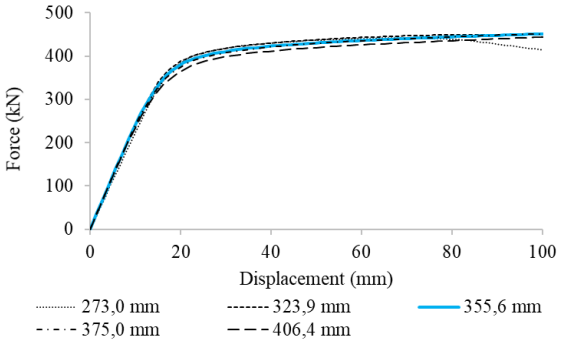

Figure 16 Vertical force-displacement curves for varying CHS column diameter (C2)

4 Conclusions

The one-way LASTTS passing-through I-beam-to-CHS joints consist of a main beam connected to one side of the tubular (CHS/SHS) column via a passing-through I-beam stub or through flange and web plates. Four parameters were analyzed for each connection configuration: C1 and C2. The C1-connection is investigated through varying the following parameters: the through I-beam section, the tube thickness, the tube diameter and the M/V ratio. The C2-connection is studied through varying the following parameters: the through flange plate thickness, the through web plate thickness, the tube thickness and the tube diameter. Based on the force-displacement curves, it can be concluded that,

- Increasing the through I-beam section (for C1) or the through flange and web plate thicknesses (for C2) increases the joint resistance.
- Increasing the tube thickness increases the joint resistance.
- The tube diameter has negligible influence on the joint resistance.
- Increasing the total beam length and therefore the M/V ratio does not have much effect on the moment resistance capacity of the joints. The influence of shear on the bending resistance of the one-way tubular joints is found to be negligible.

Different failure modes are also identified for the different configurations.

- A bending failure of the through I-beam flanges outside the tube was observed to be the most common failure for configuration C1.
- A tensile failure of the tube surface at its connection with the upper flange plate (at the front) and its connection with the lower flange plate (on the back) was observed to be the most common failure for the C2 joint configuration. However, large bending stresses in the upper flange plate just outside the CHS column and large shear stresses in the passing through web plate at the connection zone were also noticed.

Specific exceptions are also observed for some of the configurations regarding the failure modes:

- For the C1 configuration, the most notable difference was found in the models with CHS column thicknesses of 4 mm and 6 mm. The web plate failed in shear inside the CHS column along with a tensile failure of the tube surfaces at the connection zones.
- For the C2 configuration, failure in the models with thicker flange plates or thicker tubes was dominated by a shear failure of the through web plate along its connection length with the tube.

A comprehensive experimental campaign has already been planned and duly scheduled in the later half of 2023 on the one-way passing-through joints to obtain further results. Standard design guidelines will be developed, validated and disseminated in the future for the practical implementation of such joints in the construction industry.

References

[1] Wardenier, J.; Packer, J.A.; Zhao, X.L.; Van der Vegte, G.J. (2010) *Hollow sections in structural applications*. CIDECT, Geneva, Switzerland.

[2] BLM Group, All in one tube technology no: 20, Inspired Tube. (2015).

[3] Bursi, O.S. (2009) *Prefabricated composite beam-to-column filled tube or partially reinforced-concrete encased column connections for severe seismic and fire loadings*. RFSR-CT-2003-00034, Final Report.

[4] Wardenier, J.; Kurobane, Y.; Packer, J.A.; Van der Vegte, G.J.; Zhao, X.L. (2008) *Design guide for circular hollow section (CHS) joints under predominantly static loading*. CIDECT Design Guide 1.

[5] Dutta, D.; Wardenier, J.; Yeomans, N.; Sakae, K.; Bucak, O.; Packer, J.A. (1998) *Design guide for fabrication, assembly and erection of hollow section structures*. CIDECT Design Guide 7.

[6] Fukumoto, T.; Morita, K. (2005) *Elastoplastic behavior of panel zone in steel beam-to-concrete filled steel tube column moment connections*. ASCE Journal of Structural Engineering 131, 1841–1853.

[7] Sabbagh, A.B.; Chan, T.M.; Mottram, J.T. (2013) *Detailing of I-beam-to-CHS column joints with external diaphragm plates for seismic actions. Journal of Constructional Steel research* 88, 21–33.

[8] Castiglioni, C.A.; Kanyilmaz, A.; Salvatore, W.; Morelli, F.; Piscini, A.; Hjiaj, M.; Couchaux, M.; Calado, L.; Proença, J.M.; Hoffmeister, B.; Korndörfer, J.; Degee, H.; Das, R.; Raso, S.; Valli, A.; Brugnolli, M.; Galazzi, A.; Hojda, R. EU-RFCS Project LASTEICON *(Laser Technology for Innovative Joints in Steel Construction*), (2016). www.LASTEICON.EU.

[9] Kanyilmaz et al. (2021) *LASTTS: LASer cutting Technology for Tubular Structures*. EU-RFCS Project. https://www.lastts.eu/

[10] DIANA User's Manual, DIANA Release 10.2, May, 2018.

[11] Couchaux, M.; Vyhlas, V.; Hjiaj, M. (2019) *RFCS Project LASTEICON Test Report: Tests on Joints C3 and C4*. INSA, Rennes, March 2019.